Nanostructures and Thermomechanical Properties of Epoxy Thermosets Containing Reactive Diblock Copolymer

Zhiguang Xu,[1] Nishar Hameed,[1] Qipeng Guo,[1] Yiu-Wing Mai[2]

[1]*Centre for Material and Fibre Innovation, Deakin University, Geelong 3217, Victoria, Australia*
[2]*Centre for Advanced Materials Technology (CAMT), School of Aerospace, Mechanical and Mechatronic Engineering J07, University of Sydney, Sydney 2006, New South Wales, Australia*

Received 18 May 2009; accepted 11 August 2009
DOI 10.1002/app.31284
Published online 7 October 2009 in Wiley InterScience (www.interscience.wiley.com).

ABSTRACT: Polystyrene-*block*-poly(glycidyl methacrylate) reactive diblock copolymer (PS-*b*-PGMA) was synthesized via atom transfer radical polymerization (ATRP). The diblock copolymer was characterized using nuclear magnetic resonance (NMR) spectroscopy and gel permeation chromatography (GPC). The cured epoxy thermosets with 10–20 nm PS particles were prepared by blending the diblock copolymer with epoxy resin. The nanostructures were examined by means of transmission electronic microscopy (TEM) and small angle X-ray scattering (SAXS). The formation of the nanostructures was caused by the reaction-induced microphase separation mechanism. It is significant that the glass transition temperatures (T_gs) of these epoxy thermosets were increased by the addition of PS-*b*-PGMA reactive block copolymer as revealed by both differential scanning calorimetry (DSC) and dynamic mechanical analysis (DMA). © 2009 Wiley Periodicals, Inc. J Appl Polym Sci 115: 2110–2118, 2010

Key words: epoxy resin; reactive block copolymer; blends; thermomechanical properties

INTRODUCTION

The incorporation of block copolymers into thermosets, such as epoxy resin and phenolic resin is an effective way to obtain disordered (or ordered) nanostructures, which could lead to improvements in mechanical properties. Bates and coworkers[1,2] have proposed a strategy to create nanostructures in thermoset matrices via self-assembly of amphiphilic block copolymers. In this protocol, one subchain of the block copolymer cannot dissolve in the precursors for the thermosets while the others can. Hence, self-organized nanostructures, such as spherical, micelle, cylindrical, bi-continuous and lamellar structures at the nanometer scale are formed before curing. These disordered and/or ordered nanostructures can be further fixed using subsequent curing reaction. Thus in this method, the role of the curing reaction is to lock in the preformed morphology. Many researchers have studied disordered or ordered self-assembled nanostrucures in thermoset matrices with an appropriate design of block copolymer architectures.[3–25] Conversely, when all the blocks of block copolymers are miscible with the precursors of thermosets before curing polymerization but one block is immiscible with the thermoset matrix after curing, microphase separation will occur during the curing reaction. Recently, based on the above mentioned reaction-induced microphase separation mechanism, some researchers have obtained disordered (or ordered) nanostructures in the composite system of thermosets and amphiphilic block copolymers.[26–31]

Most epoxy-miscible blocks of block copolymers used to obtain nanostructures in epoxy thermosets are poly(ethylene oxide) (PEO) blocks[5–7,22,23,28] and poly(ε-caprolactone) (PCL) blocks.[25,29–31] After curing, they are miscible with the epoxy matrix via intermolecular hydrogen-bonding interactions. However, these epoxy blends have some disadvantages in mechanical properties. The glass transition temperature (T_g) and storage modulus (G') of the cured epoxy matrix, which is interpenetrated with PEO or PCL subchains of block copolymers, always decrease with increasing content of block copolymers because of the plasticization effect of the PEO or PCL blocks on epoxy.[25,28–31] To improve epoxy resins effectively, some reactive block copolymers were added to modify epoxy resins, e.g., epoxidized polystyrene-polybutadiene[26,32,33] and glycidyl methacrylate-based[11,10,34–36] block copolymers. In most of these studies, the formation of nanostructures on the addition of a reactive block copolymer has been addressed. Here, we report an increase in the glass transition temperature and the elastic modulus of the thermosets on blending with a reactive block copolymer. It should be noted that the epoxy groups of epoxidized block copolymers react with curing

Correspondence to: Q. Guo (qguo@deakin.edu.au).
Contract grant sponsors: Australian Research Council.

agents during the curing process much slower than the epoxy groups of glycidyl methacrylate (GMA) blocks of block copolymers.[11] Thus, the glycidyl methacrylate block enables the block copolymers to react quickly with the curing agent and form covalent linkages between the copolymers and the crosslinked epoxy matrix. As a result, microphase separation of the other blocks will be restricted because of strong chemical covalent interaction. It is proposed that the mechanical properties of cured epoxy thermosets containing PGMA blocks should be improved. However, studies on the morphologies and thermomechanical properties of epoxy thermosets influenced by the incorporation of reactive glycidyl methacrylate-based block copolymers remain largely unexplored.

In this work, we investigated the morphologies and thermomechanical properties of epoxy thermosets containing the reactive diblock copolymer, polystyrene-*block*-poly(glycidyl methacrylate) (PS-*b*-PGMA). These results provide an insight on how to effectively improve the mechanical properties of epoxy resins and extend the range of potential applications in various fields. First, we synthesized the diblock copolymer via atom transfer radical polymerization (ATRP) which was subsequently blended with precursors of epoxy resin to obtain nanostructures after cure. The morphologies of the cured epoxy thermosets were investigated by means of transmission electron microscopy (TEM) and small-angle X-ray scattering (SAXS), and thermomechanical properties were studied by differential scanning calorimetry (DSC) and dynamic mechanical thermal analysis (DMTA).

EXPERIMENTAL

Materials

Diglycidyl ether of bisphenol A (DGEBA) with epoxide equivalent weight of 172176 and 4,4′-methylenedianiline (MDA) curing agent were obtained from Aldrich Co. The monomers glycidyl methacrylate (GMA) and styrene (St) were also obtained from Aldrich. Before use, styrene was washed with 5% aqueous NaOH and deionized water, respectively, for three times and then distilled over CaH_2 under reduced pressure; GMA was distilled under vacuum. *N,N,N′,N″,N‴*-pentamethyldi-ethylenetriamine (PMDETA) (Aldrich, 99%), ethyl α-bromoisobutyrate (EBrIB) (Aldrich, 99%) were used as received. Copper(I) chloride (Cu(I)Cl) (Aldrich, 99.99%), copper(I) bromide (Cu(I)Br) (Aldrich, 99.99%) were purified by stirring with glacial acetic acid, then washed with acetone and dried under vacuum at room temperature. Before use, anisole (Aldrich, 99.9%) was dried by reflux over sodium/benzophenone and then distilled. All other chemicals were purchased from Aldrich.

Synthesis of polystyrene macro-initiator (PS-Br)

The polystyrene macro-initiator was synthesized via ATRP and EBrIB was used as an initiator. Degassed styrene (40.2716 g, 386.67 mmol), 40 mL of anhydrous degassed anisole, Cu(I)Br (0.3611 g, 2.52 mmol) and PMDETA (0.4363 g, 2.52 mmol) were charged to a 100 mL dried round-bottom flask equipped with a magnetic stirrer and 0.4910 g (2.52 mmol) EBrIB was added into the flask with a syringe. The system was connected to the Schlenk line system and three freeze-pump-thaw cycles were performed. The polymerization was conducted at 90°C for 8 h in an oil bath. The crude products were dissolved in dichloromethane and passed through neutral alumina column to remove the catalyst. The polymer solution was dropped into an excessive amount of cold methane and the powder obtained was dried in a vacuum oven at 30°C to constant weight. The conversion of styrene monomer was 53%.

Synthesis of polystyrene-*b*-poly(glycidyl methacrylate) (PS-*b*-PGMA) diblock copolymer

Typically, polystyrene macro-initiator (10.0757 g, 1.25 mmol), 10 mL of degassed anisole, Cu(I)Cl (0.1247 g, 1.25 mmol), PMDETA (0.1247 g, 1.25 mmol) and degassed glycidyl methacrylate monomer (9.2680 g, 65.27 mmol) were charged to a 100 mL round-bottom flask equipped with a dry magnetic stirring bar. The flask was connected to a standard Schlenk line and the mixture was degassed via three pump-freeze-thaw cycles. The flask was immersed into an oil bath at 50°C for 70 min. The crude product was dissolved in tetrahydrofuran (THF) and passed through a neutral alumina column to remove the catalyst; the polymer solution was dropped into an excessive amount of cold hexane. The PS-*b*-PGMA diblock copolymer was dried *in vacuo* at room temperature for 48 h. The polymer (18.1 g) was obtained with the conversion of glycidyl methacrylate monomer being 87%. Polymer yields were determined by gravimetry; and the molecular weight and polydispersity index were determined by gel permeation chromatography (GPC).

Preparation of epoxy thermosets containing diblock copolymer

The diblock copolymer PS-*b*-PGMA was added to the epoxy precursor DGEBA and the mixtures were acutely stirred and heated up at 100°C until the mixtures were homogenous. Then an amount of the curing agent MDA was added into the mixtures with vigorous stirring until homogeneous solutions were obtained again. It should be noted that the curing agent MDA was used in stoichiometric epoxide

(DGEBA and PGMA block)/amine ratios. The ternary mixture was poured into preheated molds and cured at 150°C for 2 h plus 180°C for 2 h for postcuring.

MEASUREMENT AND CHARECTERIZATION

Nuclear magnetic resonance spectroscopy (NMR)

The diblock copolymer was dissolved in deuterated chloroform ($CDCl_3$) and the NMR spectra were measured on a JEOL 400 MHz NMR spectrometer with tetramethylsilane (TMS) as the internal reference.

Gel permeation chromatography (GPC)

The molecular weight and molecular weight distribution of the polymer samples were measured by GPC performed on a Shimadzu system fitted with Mixed-C columns and a DRI detector. THF was used as eluent at a flow rate of 1.0 mL/min and the operations were carried out at 25°C. Molecular weights were determined from the refractive index data analyzed with Polymer Laboratories Cirrus Software, with all molecular weights being relative to polystyrene standards.

Transmission electron microscopy (TEM)

Transmission electron microscopy analyzes were performed on a JEOL JEM-2100 high resolution transmission electron microscopy at an acceleration voltage of 200 kV. The samples were trimmed at room temperature with a diamond knife using a Leica EM UC6 ultramicrotome machine. The ultrathin sections (ca. 70 nm) were collected on 400 mesh copper grids and stained with ruthenium tetroxide (RuO_4) for study.

Small-angle X-ray scattering (SAXS)

The SAXS measurements were taken on a Bruker AXS NanoStar small angle X-ray scattering instrument. Two-dimensional diffraction patterns were recorded using an image intensified CCD detector. The experiments were conducted at room temperature (25°C) using Cu Kα radiation ($\lambda = 1.54$ Å wavelength). The intensity profiles were interpreted as the plot of scattering intensity (I) versus scattering vector, $q = (4/\lambda) \sin(\theta/2)$ (θ = scattering angle).

Differential scanning calorimetry (DSC)

Calorimetric measurements were performed on a Perkin–Elmer Diamond differential scanning calorimeter in a dry nitrogen atmosphere. An indium standard was used for temperature and enthalpy calibrations. The samples (about 9.0 mg in weight) were first heated to 220°C and held at this temperature for 3 min to remove the thermal history. A heating rate of 20°C/min was used in all cases. The glass transition temperature (T_g) was taken as the midpoint of the heat capacity change.

Dynamic mechanical thermal analysis (DMTA)

The dynamic mechanical tests were performed on a dynamic mechanical thermal analyzer (DMTA) (TA Q800, USA) in a single cantilever mode under liquid nitrogen. The frequency used was 1.0 Hz and the heating rate was 3.0°C/min. The specimen dimensions were $30 \times 5.0 \times 2.0$ mm^3. The storage modulus (G'), loss modulus (G'') and tan δ were measured from −100°C to 250°C. The T_g was taken at the maximum of the tan δ curve in the glass transition region.

RESULTS AND DISCUSSION

Synthesis of reactive diblock copolymer PS-*b*-PGMA

The PS-*b*-PGMA diblock copolymer contains reactive epoxy groups at the chains of glycidyl methacrylate, which can react with the curing agent and covalently link to the epoxy matrix. The synthetic route of the reactive diblock copolymer PS-*b*-PGMA is shown in Scheme 1. The diblock copolymer PS-*b*-PGMA was synthesized via two steps of ATRP. The macro-initiator PS-Br was prepared via ATRP with ethyl α-bromoisobutyrate as initiator at 90°C for 8 h. Then PS-*b*-PGMA diblock copolymer was synthesized via ATRP with PS-Br macroinitiator. The polymerization was carried out at 50°C for 70 min in anisole solution. Here, we used the Cu(I)Cl/PMDETA catalyst system to avoid competing catalysis of epoxide polymerization of glycidyl methacrylate. ^{1}H-NMR of PS-*b*-PGMA diblock copolymer is shown in Figure 1. The simultaneous appearance of the resonance characteristics of PS and PGMA protons indicates that the diblock copolymer combined the structural

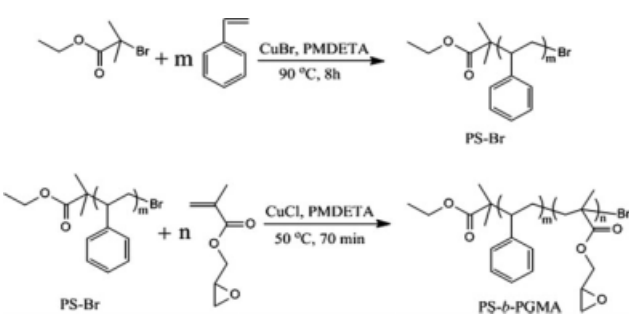

Scheme 1 Synthesis of PS-*b*-PGMA reactive diblock copolymer.

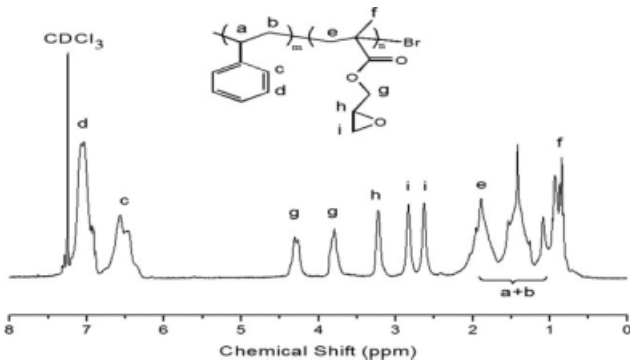

Figure 1 ^{1}H-NMR spectrum of PS-*b*-PGMA diblock copolymer.

features of PS and PGMA, which means that PS-*b*-PGMA diblock copolymer was successfully obtained. In view of the ratio of integration intensities of methyl groups of ethyl α-bromoisobutyrate to those of methylene (—CH_2—) linked with epoxy groups of PGMA blocks, the molecular weight of the diblock copolymer was calculated to be M_n = 14,200. The GPC curves of the PS macro-initiator and PS-*b*-PGMA diblock copolymer are given in Figure 2, in which the polymers display a uni-modal peak, and the molecular weight of PS-Br macro-initiator is M_n = 8,600 with a polydispersity index M_w/M_n = 1.09. The molecular weight of PS-*b*-PGMA diblock copolymer is M_n = 15,400 with M_w/M_n = 1.22. The GPC results revealed that the length of the PGMA subchain was M_n = 6,800 and the content of PS subchain was 56%.

Morphologies of epoxy thermosets containing diblock copolymer

It has been reported that the mixtures of DGEBA and PS displayed the upper critical solution temperature (UCST) behavior and the maximum critical solution temperature was around 80°C.[28,37,38] The binary mixtures of DGEBA and the homopolymer PS of the same molecular weight as the PS block were cloudy at room temperature. Upon heating, the opacity disappeared and the system became transparent at high temperature. The mixtures comprising the precursor of epoxy DGEBA, curing agent MDA and PS-*b*-PGMA diblock copolymer were transparent at the curing temperature (150°C) before being cured, suggesting that the mixtures were homogenous and no macroscopic phase separation happened at the scale more than the wavelength of visible light.

In this work, the contents of PS-*b*-PGMA diblock copolymer in epoxy thermosets varied from 10 to 40 wt %. The curing condition was 150°C for 2 h plus 180°C for 2 h. These curing temperatures were much higher than the corresponding UCST of DGEBA and PS, and the epoxy precursor and PS were miscible at this temperature, hence, there were no self-assembly structures before the curing processes. However, the PS blocks became immiscible and gradually phase separated from the cross-linked epoxy matrix during the curing reaction processing due to the driving force occurring from the reduction of entropy of mixing caused by cure polymerization. The PGMA blocks containing epoxy groups reacted with the curing agent MDA and linked with the epoxy network by chemical covalent bonding. After curing, all the samples of epoxy thermosets containing diblock copolymer remained transparent, which meant that no macro-phase separation took place during the curing process.

The morphologies of the cured epoxy containing the reactive diblock copolymer PS-*b*-PGMA were examined by transmission electron microscopy (TEM) and small-angle X-ray scattering (SAXS). Specimens of epoxy containing diblock copolymer for TEM analysis were microtomed and the thickness was ~70 nm. The specimens were then stained with RuO_4 vapor and the PS domains would be stained to black while the aromatic epoxy thermoset matrix appeared gray. The TEM images of epoxy thermosetting containing 10, 20, 30, and 40 wt % of PS-*b*-PGMA diblock copolymer are shown in Figure 3. In these images, the light continuous regions are the cross-linked epoxy matrix, which was covalently linked to the reactive PGMA blocks of the diblock copolymer, while the dark regions are PS domains. It is noted that all epoxy thermosets containing the diblock copolymer possess nanostructured morphologies. As shown in Figure 3(a), the spherical particles with an average size of 20–30 nm were uniformly dispersed in the continuous cross-linked epoxy matrix, which indicate that micro-phase separation of diblock copolymer occurred during the curing processes. When the PS-*b*-PGMA diblock copolymer content exceeds 10 wt % the density of PS domains increases and the shape changes to worm-like morphologies. From Figures 3(b–d), it can be seen that with increasing content of diblock

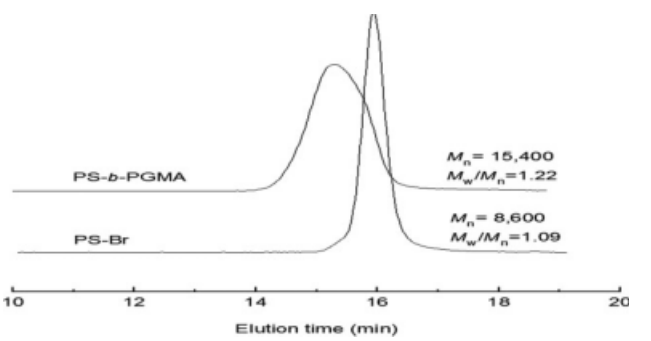

Figure 2 GPC curves of PS-Br macro-initiator and PS-*b*-PGMA diblock copolymer.

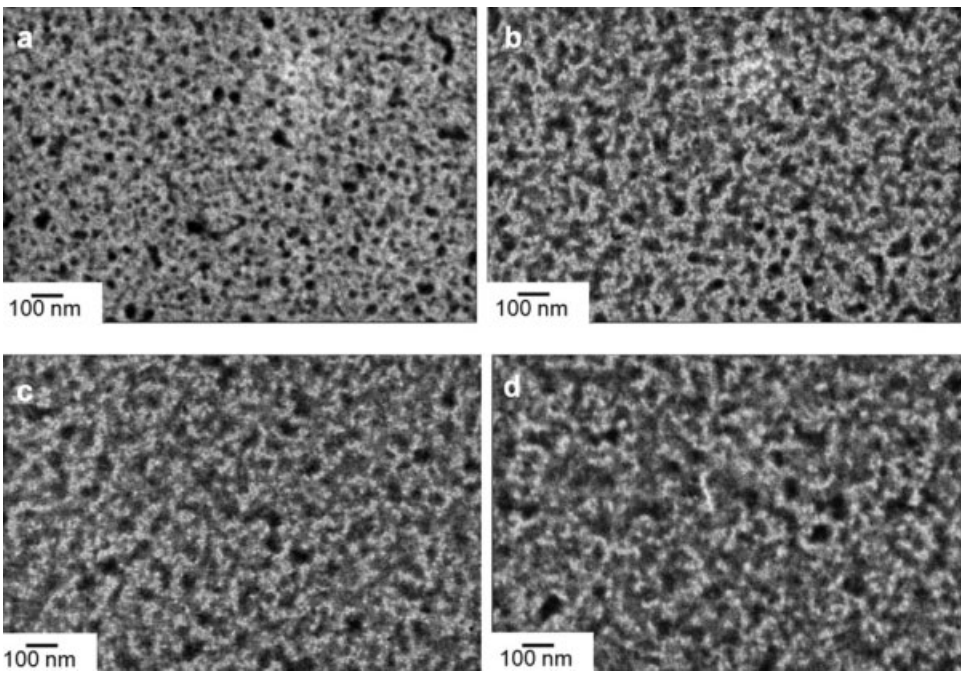

Figure 3 TEM images of epoxy thermosets containing (a) 10, (b) 20, (c) 30, and (d) 40 wt % of PS-*b*-PGMA diblock copolymer.

copolymer, the PS domain density increases. These results were also confirmed by small-angle X-ray scattering (SAXS) as discussed later.

The morphologies of the epoxy thermosets containing reactive diblock copolymer were further investigated by small-angle X-ray scattering (SAXS). Shown in Figure 4 are the SAXS profiles of cured epoxy thermosets. Here, well-defined scattering peaks are seen in all cases, indicating that micro-phase separation at the nanometer scale has occurred in the epoxy thermosets containing PS-*b*-PGMA diblock copolymer. As the diblock copolymer content is increased, the positions of the scattering maxima remain essentially constant, apart from slight shifts to higher q values. Based on the positions of the primary scattering peaks, the average distance ($L = 2\pi/q_m$) between neighboring PS domains are calculated to be 29.4, 25.6, 23.7, and 22.9 nm for the epoxy thermosets containing PS-*b*-PGMA diblock copolymer of 10, 20, 30 and 40 wt %, respectively. It is noted that L between the neighboring PS domains decreases with increasing content of the PS-*b*-PGMA diblock copolymer. The density of PS domains becomes higher as the content of diblcok copolymer in the epoxy matrix increases, which results in reduced distance between the PS domains. These results are in a good agreement with those obtained from TEM, Figure 3.

It should be noted that the morphology of epoxy thermosets containing PS-*b*-PGMA reactive diblock copolymer is different from those of epoxy thermosets with nonreactive amphiphilic diblock copolymer poly(ethylene oxide)-*block*-polystyrene (PEO-*b*-PS)[28] and poly(caprolactone)-*block*-polystyrene (PCL-*b*-PS),[31] which have molecular weights comparable to the PS subchain of PS-*b*-PGMA diblock copolymer. The microphase separation of PS blocks occurred during

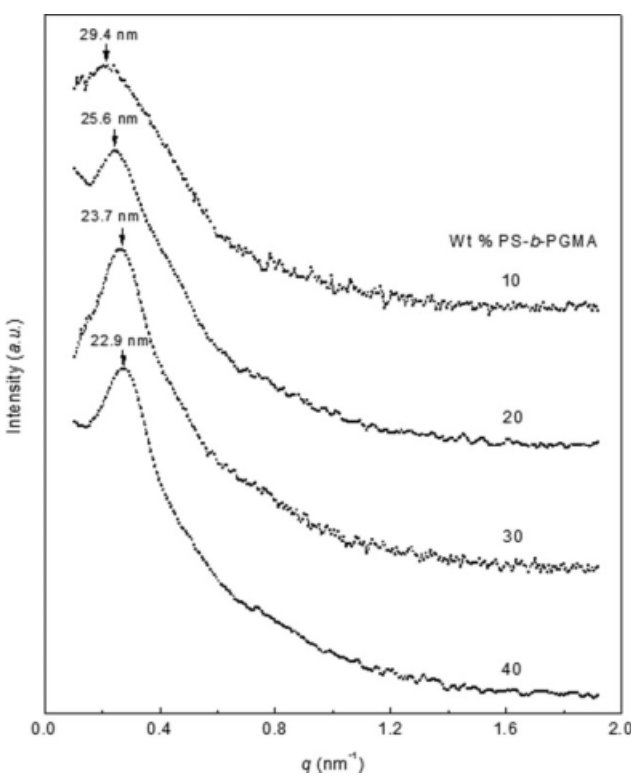

Figure 4 SAXS profiles of epoxy thermosets containing PS-*b*-PGMA diblock copolymer. Each profile is shifted vertically for clarity.

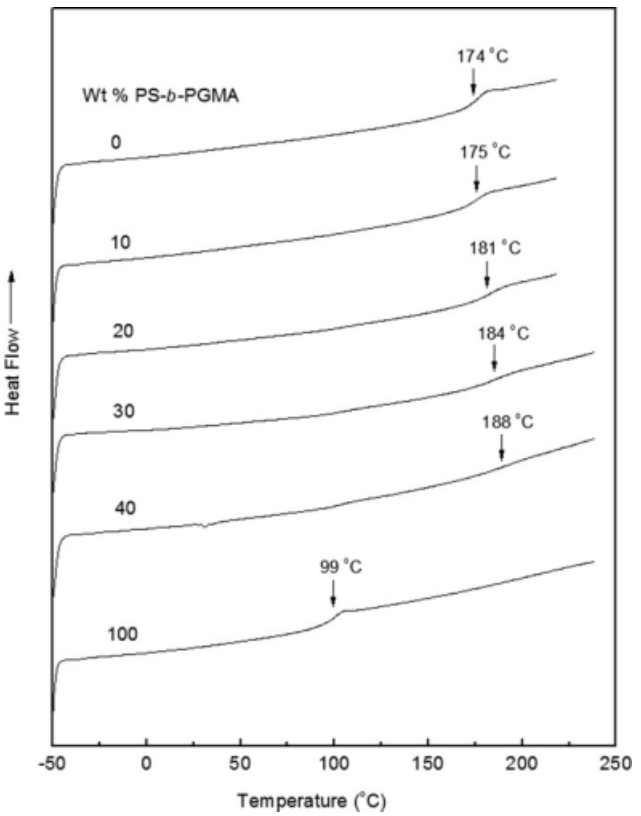

Figure 5 DSC curves of PS-*b*-PGMA diblock copolymer, neat epoxy and nanostructured epoxy thermosets containing the diblock copolymer.

curing processes and formed nanostructures with 10–20 nm particles in epoxy thermosets in these latter systems containing nonreactive block copolymers. The nanoparticles can form ordered nano-structures when the concentration of the diblcok copolymer PEO-*b*-PS or PCL-*b*-PS is 30 wt % or more, while the system containing PS-*b*-PGMA diblock copolymer obtains disordered nanostructures in epoxy matrix even the content of PS-*b*-PGMA is up to 40 wt %. Both PEO and PCL blocks are miscible with epoxy thermosets because of the formation of the intermolecular hydrogen bonding interactions between the aromatic amine cross-linked epoxy matrix and PEO or PCL blocks. PGMA containing epoxy groups can react with the curing agent and link with the epoxy network via chemical covalent bonding interactions. Such covalent interactions, which restrict PS microphase separation, are stronger than the intermolecular hydrogen bonding interactions. Thus, the PS microdomains were restricted and formed disordered nanostructures in the epoxy thermosets.

Thermomechanical properties of nanostructured epoxy resin

Reactive PGMA blocks can react with the curing agent and form covalent bonding with the epoxy networks, thus the nanostructured epoxy thermosets should possess interesting thermal properties. We have investigated the thermomechanical properties of these nanostructured epoxy thermosets by means of DSC and DMTA. The DSC curves of neat epoxy resin, nanostructured epoxy thermosets and PS-*b*-PGMA reactive diblock copolymer are shown in Figure 5. Plain PS-*b*-PGMA diblock copolymer displays a glass transition at ~100°C, which is due to the glass transition of PS subchain of the diblock copolymer. The glass transition temperature (T_g) of the neat epoxy is *c.a.* 174°C, and the T_gs of nanostructured epoxy thermosets containing 10, 20, 30 and 40 wt % reactive diblock copolymer PS-*b*-PGMA are *c.a.* 175, 181, 184 and 188°C, respectively. As shown in Figure 6, it is interesting that the T_gs of the nanostructured epoxy thermosets increase with increasing content of PS-*b*-PGMA diblock copolymer. This observation is different to previous nanostructured aromatic amine-cured epoxy systems[21–25,27–31] containing PEO/PCL blocks, where the T_gs of nanostructured epoxy thermosets decreased with increasing concentration of block copolymers. It could be attributed to the plasticization of the soft PCL/PEO chains which were incorporated in the cross-linked epoxy matrices by hydrogen-bonding interactions. The introduction of PS-*b*-PGMA reactive diblock copolymer into epoxy resin can increase significantly the T_gs of the cured epoxy thermosets, which may improve the mechanical properties. It must be pointed out that the glass transition observed in the present temperature range is ascribed to the epoxy matrix that is

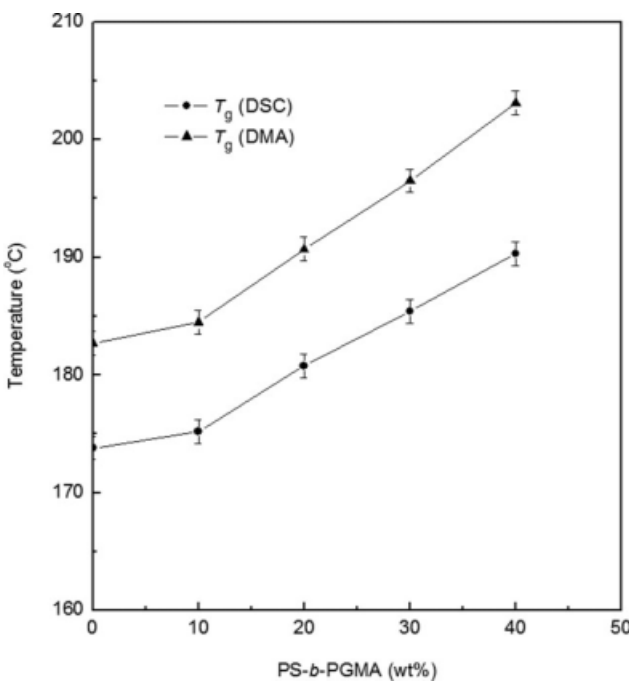

Figure 6 T_g values of cured epoxy thermosets obtained by DSC and DMA.

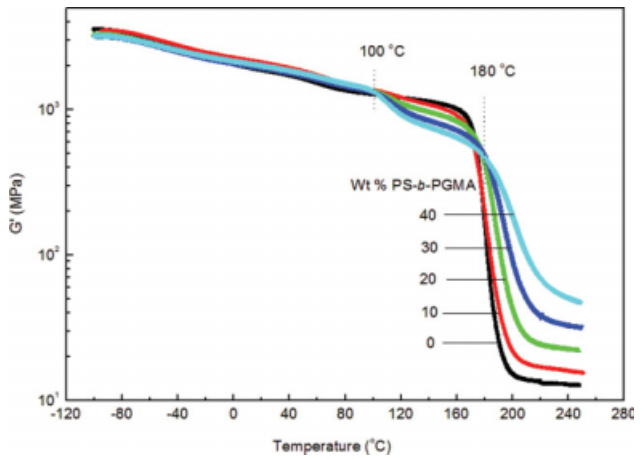

Figure 7 Storage modulus (G') *versus* temperature curves of neat epoxy and nanostructured epoxy thermosets containing 10, 20, 30, and 40 wt % PS-*b*-PGMA diblock copolymer. [Color figure can be viewed in the online issue, which is available at www.interscience.wiley.com.]

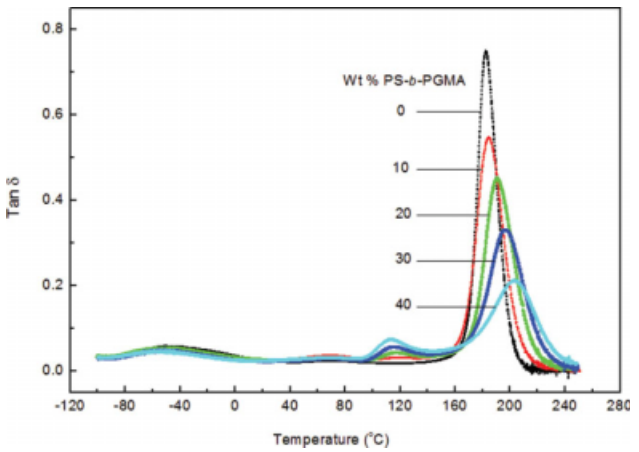

Figure 8 Tan δ *versus* temperature curves of neat epoxy and nanostructured epoxy thermosets containing 10, 20, 30, and 40 wt % PS-*b*-PGMA diblock copolymer. [Color figure can be viewed in the online issue, which is available at www.interscience.wiley.com.]

covalently linked to the reactive epoxy groups of the PGMA subchain of the diblock copolymer. The crosslink density of the nanostructured epoxy network is improved due to the increasing concentration of PGMA sub-chains in epoxy matrix. So the glass transition region moves to higher temperatures because of the higher cross-link density.[39,40]

Figure 7 shows the storage modulus (G') *versus* temperature curves of neat epoxy and nanostructured epoxy thermosets. Obviously, the storage moduli of neat epoxy and nanostructured epoxies show little change below 100°C. When the temperature is within the range 100 and 180°C, G' of the nanostructured epoxy resins decreases with increasing content of PS-*b*-PGMA diblock copolymer. This is ascribed to the increase of PS domains in epoxy matrix. This is further evidenced in Figure 8. However, G' of nanostructured epoxy thermosets increases rapidly with increasing content of diblock copolymer above 180°C, a result that is important to extend the range of potential applications of PS-*b*-PGMA diblock copolymer-based epoxy at high temperatures. Tan δ *versus* temperature curves are shown in Figure 8 whereby the relaxation peaks, corresponding to the glass transitions of the epoxy thermosets, are displayed. For neat epoxy, there is a well-defined major relaxation peak at 183°C due to the glass-rubber transition (viz. α-transition) mechanism. Besides the α transition, MDA-cured neat epoxy resin exhibits secondary transitions (viz. β-relaxation) at the lower temperature (ca. −50°C). This transition is attributed predominantly to the motion of the hydroxyl ether structural units [CH_2—CH(OH)—CH_2—O—] and the diphenyl groups in amine-crosslinked epoxy. The T_gs of epoxy thermosets containing 10, 20, 30 and 40 wt % PS-*b*-PGMA diblock copolymer are 185, 191, 197, and 203°C, respectively. It is noted that the T_gs of the nanostructured epoxy thermosets containing reactive diblock copolymer are higher than that of neat epoxy, and the T_gs increase with increasing PS-*b*-PGMA diblock copolymer content. The T_gs of cured epoxy thermosets obtained by DSC and DMA are summarized in Figure 6, whereby we can see that the T_g values from DMA are generally 10°C higher than those from DSC as expected.[41,42] The T_gs of nanostructured epoxies are significantly increased due to the incorporation of PGMA block-based reactive diblock copolymer such that the PGMA subchain of the block copolymer reacts with the epoxy, hence increasing the crosslink density of the epoxy matrix network. It can be seen in Figure 8 that, upon incorporating PS-*b*-PGMA reactive diblock copolymer into the epoxy thermosets, new transitions appear around 115°C besides the α- and β-relaxations assignable to the epoxy matrix. Figure 9 shows the expanded tan δ versus temperature of neat epoxy resin and nanostructured epoxy resin in the range of 80 – 150°C. We can see clearly that the intensity of the peaks increases with increasing concentration of the PS-*b*-PGMA diblock copolymer. The new peaks can be assigned to the glass transition of the PS domains in the nanostructured epoxy thermosets, which goes up with increasing concentration of PS microphase domains in epoxy. It has been proven that PS and epoxy precursors showed an UCST behavior and that reaction-induced microphase separation of PS-*b*-PGMA diblock copolymer occurred during curing of diblock copolymer-based epoxy blends. The DMTA results in Figure 9 confirm that the PS domains form *via* reaction-induced micro-phase separation in the epoxy matrix.

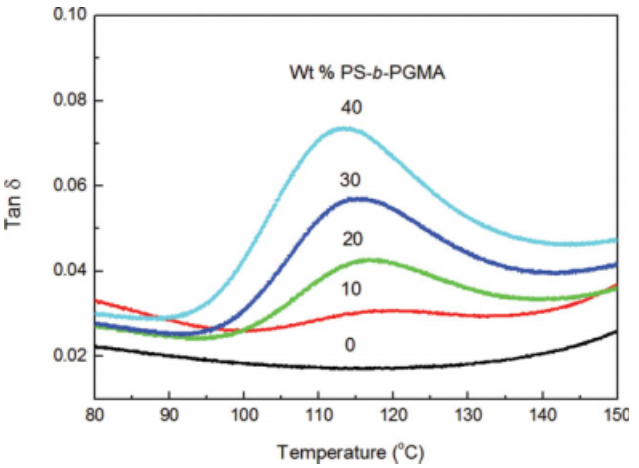

Figure 9 Expanded tan δ *versus* temperature curves of neat epoxy and nanostructured epoxy thermosets containing PS-*b*-PGMA diblock copolymer in the range of 80–150°C. [Color figure can be viewed in the online issue, which is available at www.interscience.wiley.com.]

The reactivity difference between DGEBA and PGMA with amine-containing curing agents was investigated by Rebizant et al.[10] They found that the reaction rate of DGEBA is about 3 times that of PGMA at low conversions, and that this behavior is reversed beyond 50% conversion, with a higher reaction rate for PGMA. The addition of PS-*b*-PGMA diblock copolymer results in an increase in T_g of the thermosets. Incorporation of a higher functionality cross-linker or an inorganic filler material could achieve a similar effect. Although a 10–20°C improvement in T_g is not outstandingly high considering it requires 40 wt % block copolymer, the enhanced G' values above T_g could be gainfully exploited for high-temperature applications.

CONCLUSION

Reactive diblock copolymer PS-*b*-PGMA comprising epoxy groups was synthesized via ATRP and characterized by ^{1}H-nuclear magnetic resonance spectroscopy (NMR) and GPC. Nanostructured epoxy resins were obtained from the mixtures of epoxy and reactive diblock copolymer via reaction-induced microphase separation. Transmission electron microscopy (TEM) and small-angle X-ray scattering (SAXS) results show that 10–20 nm PS particles were dispersed in the epoxy matrix and the distance between the PS microphase decreased with increasing diblock copolymer content. The incorporation of epoxy groups in PS-*b*-PGMA diblock copolymer restricted microphase separation of the PS blocks and formed disordered nanostructures. It is noted that the T_g values of these nanostructured epoxies were increased by incorporating the PS-*b*-PGMA reactive diblock copolymer because of the covalent linkages between PS microphase of the diblock copolymer and the cross-linked epoxy network. Moreover, the storage moduli (G') of the nanostructured epoxy resins were greatly improved with increasing content of diblock copolymer above the T_g of neat epoxy resin. The introduction of the reactive diblock copolymer containing PGMA blocks in epoxy thermosets is expected to increase the mechanical properties which are under investigation.

The authors thank Dr. Aravind Dasari (IDMEA, Madrid, Spain) for the GPC measurements.

References

1. Hillmyer, M. A.; Lipic, P. M.; Hajduk, D. A.; Almdal, K.; Bates, F. S. J Am Chem Soc 1997, 119, 2749.
2. Lipic, P. M.; Bates, F. S.; Hillmyer, M. A. J Am Chem Soc 1998, 120, 8963.
3. Francis, B.; Thomas, S.; Jose, J.; Ramaswamy, R.; Rao, V. L. Polymer 2005, 46, 12372.
4. Francis, B.; Rao, V. L.; Poel, G. V.; Posada, F.; Groenincks, G.; Ramaswamy, R.; Thomas, S. Polymer 2006, 47, 5411.
5. Mijovic, J.; Shen, M.; Sy, J. W.; Mondragon, I. Macromolecules 2000, 33, 5235.
6. Guo, Q.; Thomann, R.; Gronski, W.; Thurn-Albrecht, T. Macromolecules 2002, 35, 3133.
7. Guo, Q.; Thomann, R.; Gronski, W.; Staneva, R.; Ivanova, R.; Stühn, B. Macromolecules 2003, 36, 3635.
8. Ritzenthaler, S.; Court, F.; Girard-Reydet, E.; Leibler, L.; Pascault, J. P. Macromolecules 2002, 35, 6245.
9. Ritzenthaler, S.; Court, F.; Girard-Reydet, E.; Leibler, L.; Pascault, J. P. Macromolecules 2003, 36, 118.
10. Rebizant, V.; Abetz, V.; Tournihac, T.; Court, F.; Leibler, L. Macromolecules 2003, 36, 9889.
11. Grubbs, R. B.; Dean, J. M.; Broz, M. E.; Bates, F. S. Macromolecules 2000, 33, 9522.
12. Kosonen, H.; Ruokolainen, J.; Nyholm, P.; Ikkala, O. Macromolecules 2001, 34, 3046.
13. Kosonen, H.; Ruokolainen, J.; Nyholm, P.; Ikkala, O. Polymer 2001, 42, 9481.
14. Rebizant, V.; Venet, A. S.; Tournillhac, F.; Girard-Reydet, E.; Navarro, C.; Pascault, J. P.; Leibler, L. Macromolecules 2004, 37, 8017.
15. Könczöl, L.; Döll, W.; Buchholz, U.; Mülhaupt, R. J Appl Polym Sci 1994, 54, 815.
16. Wu, J.; Thio, Y. S.; Bates, F. S. J Polym Sci Part: B Polym Phys 2005, 43, 1950.
17. Dean, J. M.; Verghese, N. E.; Pham, H. Q.; Bates, F. S. Macromolecules 2003, 36, 9267.
18. Dean, J. M.; Grubbs, R. B.; Saad, W.; Cook, R. F.; Bates, F. S. J Polym Sci Part: B Polym Phys 2003, 41, 2444.
19. Guo, Q.; Dean, J. M.; Grubbs, R. B.; Bates, F. S. J Polym Sci Part: B Polym Phys 2003, 41, 1994.
20. Maiez-Tribut, S.; Pascault, J. P.; Soule, E. R.; Borrajo, J.; Williams, R. J. J. Macromolecules 2007, 40, 1268.
21. Sinturel, C.; Vayer, M.; Erre, R.; Amenitsch, H. Macromolecules 2007, 40, 2532.
22. Guo, Q.; Chen, F.; Wang, K.; Chen, L. J Polym Sci Part: B Polym Phys 2006, 44, 3042.
23. Guo, Q.; Wang, K.; Chen, L.; Zheng, S.; Halley, P. J. J Polym Sci Part: B Polym Phys 2006, 44, 975.
24. Guo, Q.; Liu, J.; Chen, L.; Wang, K. Polymer 2008, 49, 1737.
25. Ocando, C.; Serrano, E.; Tercjak, A.; Peña, C.; Kortaberria, G.; Calberg, C.; Grignard, B.; Jerome, R.; Carrasco, P. M.;

Mecerreyes, D.; Mondragon, I. Macromolecules 2007, 40, 4068.
26. Larrañaga, M.; Gabilondo, N.; Kortaberria, G.; Serrano, E.; Remiro, P.; Riccardi, C. C.; Mondragon, I. Polymer 2005, 46, 7082.
27. Serrano, E.; Tercjak, A.; Kortaberria, G.; Pomposo, J. A.; Mecerreyes, D.; Zafeiropoulos, N. E.; Stamm, M.; Mondragon, I. Macromolecules 2006, 39, 2254.
28. Meng, F.; Zheng, S.; Li, H.; Liang, Q.; Liu, T. Macromolecules 2006, 39, 5072.
29. Xu, Z.; Zheng, S. Polymer 2007, 48, 6134.
30. Xu, Z.; Zheng, S. Macromolecules 2007, 40, 2548.
31. Meng, F.; Xu, Z.; Zheng, S. Macromolecules 2008, 41, 1411.
32. Serrano, E.; Martin, M. D.; Tercjac, A.; Pomposo, J. A.; Mecerreyes, D.; Mondragon, I. Macromol Rapid Commun 2005, 26, 982.
33. Serrano, E.; Larrañaga, M.; Remiri, P. M.; Mondragon, I.; Carrasco, P.; Pomposo, J. A.; Mecerreyes, D. Macromol Chem Phys 2004, 205, 987.
34. Grubbs, R. B.; Broz, M. E.; Dean, J. M.; Bates, F. S. Macromolecules 2000, 33, 2308.
35. Grubbs, R. B.; Dean, J. M.; Bates, F. S. Macromolecules 2001, 34, 8593.
36. He, S.; Wang, X.; Guo, X.; Shi, K.; Du, Z.; Zhang, B. Polym Int 2005, 54, 1543.
37. Hoppe, C. E.; Galante, M. J.; Oyanguren, P. A.; Williams, R. J. J.; Girard-Reydet, E.; Pascault, J. T. Polym Eng Sci 2002, 42, 2361.
38. Zucchi, I. A.; Galante, M. J.; Borrajo, J.; Williams, R. J. J. Macromol Chem Phys 2004, 205, 676.
39. Pascault, J. P.; Williams, R. J. J. J Polym Sci Part: B Polym Phys 1990, 28, 85.
40. Hale, A.; Macosko, C. W.; Bair, H. E. Macromolecules 1991, 24, 2610.
41. Guo, Q.; Huang, J.; Chen, T.; Zhang, H.; Yang, Y.; Hou, C.; Feng, Z. Polym Eng Sci 1990, 30, 44.
42. Guo, Q.; Slavov, S.; Halley, P. J. J Polym Sci Part: B Polym Phys 2004, 42, 2833.